Performance and dynamic modelling of mixed biomass-kaolin packed bed adsorption column for the removal of aqueous phase methylene blue (MB) dye

Alison Shak, Sara Dawood, Tushar Kanti Sen*

*Department of Chemical Engineering, Curtin University, GPO Box U1987, 6845 Western Australia, Australia,
email: pohjik.shak@graduate.curtin.edu.au (A. Shak), sara.dawood@postgrad.curtin.edu.au (S. Dawood),
Tel. No. +61892669052, email: t.sen@curtin.edu.au (T.K. Sen)*

ABSTRACT

This present study evaluates the adsorptive effectiveness of mixed pine cone biomass and kaolin clay adsorbents in removing methylene blue (MB) dye from its aqueous solution using a packed-bed column adsorption experiment. A series of column experiments were performed to determine the breakthrough curves (BTCs) by varying bed height, inlet feed flow rate and initial MB dye inlet concentration and various characteristic parameters such as % removal of dye, initial breakthrough time, used bed length and unused bed length, mass transfer zone (MTZ) and dye adsorption density (q_{total}) were determined here. The adsorption of MB dye was found most favourable under low feed flow rate, high adsorbent bed height and high initial MB dye concentrations. Four kinetic column models, namely Thomas, Yoon-Nelson, Clarkand Bed Depth Service Time (BDST) were fitted against the experimental data to predict the column breakthrough curves (BTC) behaviour under different operational conditions. All models were found suitable in describing the dynamic behaviour of the column. The various adsorptive kinetic parameters such as rate constant, the adsorption capacity for Thomas model, the time for 50% breakthrough in Yoon-Nelson model, Clark constants, the service time for BDST model and unused bed are determined and critically analysed which are useful for designing the large-scale column operation. This continuous column study revealed the strong ability of mixed pine cone biomass and kaolin clay packed bed adsorbents to remove the dye and other pollutants and may be recognised as an alternative sustainable solution for dye-bearing wastewater treatment in industrial scale.

Keywords: Methylene blue (MB); Adsorption; Fixed-bed column; Thomas; Yoon-Nelson; BDST; Clark; Pine cone biomass; Kaolin; Adsorbent

1. Introduction

Water is an essential aspect in maintaining the life of people, plants and animals. The quality of water is deteriorating day by day due to urbanization, industrialization, population growth and human activities. Water pollution due to presence of toxic inorganics and organics is one of the important present day issue causing serious problems to living beings. One of the major source of water pollution is industrial effluents and industries such as paper, food, plastic and textile are among those industries which gen-

erated large volume of dye bearing effluents [1–3]. It has been reported that more than 100,000 commercial dyes are known with an annual production of 7×10^5 ton/y. The total consumption of dyes in textile industries worldwide is more than 10,000 ton/y and approximately 100 ton/y of dyes are discharged into the water body [4–6]. Basically 10–25% materials are lost during the dying process due to technical inefficiencies and roughly 2–20% of it is directly discharged as effluents to the environment [7]. Dyes are considered as potential pollutants because they are toxic in nature [8]. Dyes have the ability to reduce penetration of sunlight, increases the occurrence of eutrophication and interference with receiving water ecology. In addition, it also decreases the photosynthesis of aquatic plants [9–11]. Methylene

*Corresponding author.

blue is the most common substance used for dying cotton, wood and silk. Even though methylene blue is known to be not strongly hazardous, it can still cause some harmful effects under acute exposure. Methylene blue may cause an increased in heart rate, vomiting, shock, cyanosis, jaundice, and quadriplegia and tissue necrosis in humans [12].

Various dye bearing effluents treatment methods like membrane process, adsorption, ozonation [13], oxidation [14], photocatalytic reduction [15] and coagulation/flocculation [16] have been reported with varying degree of success [3–5,8,17]. Among these adsorption is the most favoured separation technique for inorganic and organic bearing effluents, because of its simple in operation, low-cost, availability, efficiency and effectiveness [18–21]. Commercial activated carbon (CAC) is the most effective adsorbents in the removal of inorganics and organics but its high cost, regeneration difficulties and disposal problems makes restricted in wastewater treatment application [3,6,19]. Therefore, today researchers are trying to find alternative low cost adsorbents from agricultural and industrial solid waste. It has two-fold benefits, one utilization of cost-effective alternative adsorbents and secondly, efficient management of large solid waste disposal problem.

In recent years there are large number of reported results on low cost alternative adsorbents such as pine cone [21], Eucalyptus wood [22], Eucalyptus bark [23], pine cone based activated carbon [18], Eucalyptus bark based bio-char [5], tea waste carbon [24], montmorillonite [25], zeolite [26,27], kaolin [27–31], bentonite [32,33], chitosan [34,35] and their ability to remove dye and metal ions from water and wastewater. The main components of biomass waste materials are hemicelluloses, lignin, lipids, proteins, water, hydrocarbons and starch which are responsible for good capacity adsorbent. Sea by-product such as chitosan consists mainly of lignin and cellulose. Lignin has polar functional groups that can be involved in chemical bonding thus it can be used effectively in the removal of a variety of pollutants [3]. Readers are encouraged to go through couple of recently published review articles on compilation of low-cost sorbents for metal and dye bearing wastewater treatment [3,19,36,37,2,21]. Clay minerals have both negative and positive charges on the surface thus enhance the adsorption process for cationic and anionic dyes [6]. However, most of these investigations were restricted to the batch equilibrium studies and limited to single adsorbent system. In this present study, the effectiveness of mixture of pine cone biomass and kaolin clay minerals in the removal of methylene blue (MB) dye from its aqueous phase has been tested through fixed bed adsorption column operation. To become more feasible option for large scale adsorption process for dye bearing effluent treatment, we have selected the mixture of clay minerals and biomass based mixed adsorbents through column operation mode. Batch equilibrium experiment provides useful information on the effectiveness of adsorbents under different physio-chemical process conditions. Besides that, it also provides the information on the dye adsorption mechanism and kinetic parameters needed to optimise an adsorption process [38]. However the data may not be applicable to most of the actual treatment system (such as continuous column operation) where contact time is not sufficient for the attainment of equilibrium and existence of many undesirable mass transfer phenomena. Thus, it is not easy to apply batch experimental data directly to a fixed-bed column performance because isotherms are incapable of providing accurate data for scale up purposes. Hence, there is an urge to determine the adsorption capacity for an adsorbent mixture of more than one adsorbent under continuous column operation. To the best of our knowledge, no other research group has done any work with a mixed adsorbent filled packed column to remove MB dye from wastewater. Therefore the aim of this study is also to investigate the effects of process parameters such as inlet flow rate, bed depth and initial methylene blue concentration on adsorption capacity of mixed adsorbent in a dynamic packed-bed column operation. Finally, the breakthrough curves have been analysed using Thomas, Yoon-Nelson and Bed Depth Service Time (BDST) and Clark kinetic models for the column performance.

2. Materials and methods

2.1. Packed bed mixed adsorbents

Pine cone biomass and kaolin clay minerals both are used in this present study. Pine cones biomass were collected locally between May to June from Curtin University Bentley Campus, Perth, Western Australia, Australia. Initially raw biomass was washed several times using distilled water to remove any impurities, followed by drying in an oven at 75°C for 24 h. The dried pine cones were smashed using a grinder and screened using a 106 μm British Standard Sieve. Particles larger than 106 μm were further crushed in the grinder until all particles have passed through the sieve mesh. Particles were collected in plastic containers and labelled accordingly. The pine cone particles were rewashed with deionized water at 30°C and stirred for 30 min with a magnetic stirrer to remove its natural dye content. Washing of the pine cone particles were repeated until the most of the inherent natural dye from pine cones were removed. Meanwhile, Kaolin was obtained from Ajax Finecham Pty. Ltd. Australia and dried in an oven at 70°C for 24 h before use. Then the packed bed mixed adsorbent materials were prepared by mixing with dried pine cone particles and kaolin clay minerals at an optimum mixing ratio. The most suitable mixture ratio of pine cone to kaolin was determined from batch adsorption experiments at different mass ratios. The functional groups present in the adsorbent mixture before and after adsorption were identified using a spectrum 100 FTIR spectrophotometer. The particle sizes of pine cone and kaolin adsorbent mixture was measured using the Malvern Hydro 2000s Master Sizer (Malvern Instruments Ltd., UK).

2.2. Adsorbate and concentration measurement

Cationic dye MB was selected as an adsorbate for this study. The molecular formula of methylene blue is $C_{16}H_{18}N_3$ SCI with a molecular weight of 319.65 g/gmol and its chemical structure as shown in Fig. 1 [39].

MB of analytical grade supplied by Sigma-Aldrich Pty. Ltd. was used in this study. MB stock solution of 1000 mg/L was prepared by dissolving appropriate amount of dye
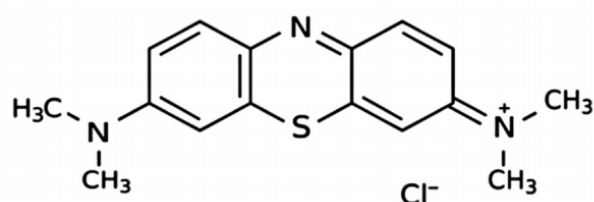
Fig. 1. Molecular Structure of Methylene Blue [40].

into deionised water of a 1 L volumetric flask. The various experimental solution were prepared by diluting the stock solution with deionised water to give the desired concentration. The concentration of MB solution was measured by SP-8001 UV/visible spectrophotometer (Perkin Elmer, USA). The calibration curve for methylene blue dye solution was plotted based on measured MB dye concentrations using UV Spectrophotometer at a maximum wavelength of 668 nm. This calibration curve was used as reference in determining the unknown concentration of each MB dye during column adsorption operation

2.3. A continuous adsorption study in a packed-bed column

The continuous flow packed-bed column adsorption experiments were conducted in a vertical perspex glass column with an internal diameter of 2.5 cm and height of 30 cm which is shown in Fig. 2. The column was packed with the adsorbent mixture of known quantity to the desired height of 3, 5 and 7 cm in between two supporting layers of pre-equilibrated glass wool to ensure a securely packed arrangement as shown in Fig. 2. Circular threaded caps were used to enclose both ends of the column. A variable speed peristaltic pump (supplied by ProMinent Fluid Controls, NSW, and Australia) was placed at the bottom of the packed bed column to inject influent MB dye solution into the column at a constant discharge rate. The column experiments were conducted at room temperature without any pH adjustments. The effect of mixed adsorbent bed height (3, 5 and 7 cm), feed flow rate (13, 15 and 17 mL/min) and initial MB concentration (50, 100 and 150 ppm) on break-through-curves (BTCs) were investigated. The adsorption of MB was conducted at neutral pH as it is proven to have the best removal status in this condition [39]. Effluent samples were collected at specific time intervals and the concentration of MB were measured using the UV Spectrophotometer. The BTCs obtained under various process conditions were fitted against different column kinetic and mass transfer models and the respective model parameters were calculated. All the experimental measurements are in general reproducible within ± 10% accuracy.

2.4. Modelling and adsorption column data analysis

2.4.1. Theory of breakthrough curve (BTC) and mass transfer zone (MTZ)

The theory of Breakthrough Curve (BTC) was used in analysing the adsorption performance of a packed-bed column. The shape of a BTC and its breakthrough time
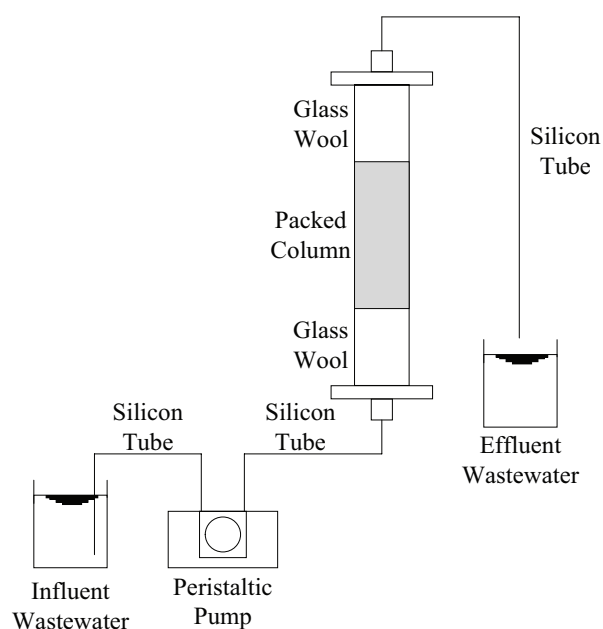
Fig. 2. Schematic diagram of packed bed column.

are important characteristics in evaluating the dynamic behaviour of an adsorption column [41]. Thus, the prediction of a concentration-time profile based on the column effluent from BTC is required in designing a suitable adsorption column. Adsorption performance is dependent on the feed flow rates, initial dye concentration and bed depth. A typical BTC is usually expressed by a $C_{effluent}$ (C_t)/ $C_{influent}$ (C_o) versus volume of effluent or service time plot for a given bed height as shown in Fig. 3 [8].

The following parameters are calculated for column data analysis The time equivalent to total or stoichiometric capacity is calculated using the following equation [38]

$$t_t = \int_{t=0}^{t=\infty}\left(1 - \frac{C_t}{C_o}\right)dt = A_1 + A_2 \tag{1}$$

Time equivalent to usable capacity is determined using Eq. (2) [38].

$$t_u = \int_{t=0}^{t_b}\left(1 - \frac{C_t}{C_o}\right)dt = A_1 \tag{2}$$

The usable capacity of bed up to the breakthrough time point t_b and A_2 area calculation the height of unused bed.

$$t_u \approx t_b$$

Area under the curve as per Eq. (1) gives the total time value, while the area under the curve as per Eq. (2) gives usable capacity time. The area under the curve can be determined using graphical method or by numerical integration. The fraction of the total bed capacity or length utilized up to the break point is expressed as t_u/t_t. The height of the unused bed (HUNB) or Mass Transfer Zone (MTZ) is calculated using Eqs. (3) and (4) [38].
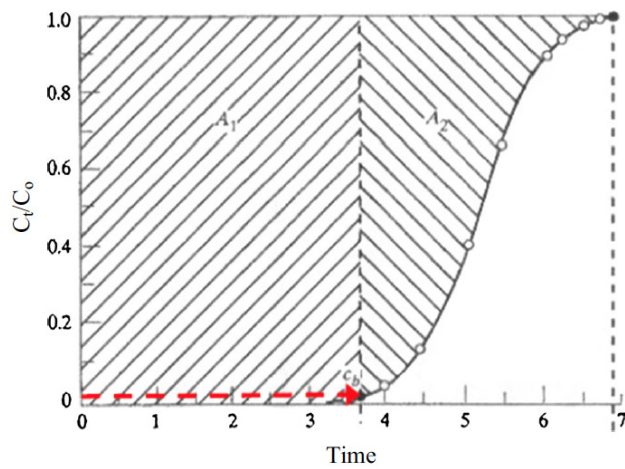
Fig. 3. Ideal breakthrough curve [8].

$$H_{UNB} = \left(1 - \frac{t_u}{t_t}\right) H_T = \left(1 - \frac{t_b}{t_t}\right) H_T \qquad (3)$$

$$MTZ = H_{UNB} \qquad (4)$$

where H_T = total bed height (cm)

The used bed length up to the break point H_B is calculated using Eq. (5) [38].

$$H_B = \left(\frac{t_b}{t_t}\right) H_T \qquad (5)$$

The total effluent volume V_{eff} is estimated using Eq. (6) [38].

$$V_{eff} = Q \cdot t_{total} \qquad (6)$$

where Q = volumetric glow rate (mL/min) and t_{total} = total flow time (min).

The BTC plot can be used to find the total quantity of methylene blue adsorbed. The total amount of methylene blue adsorbed in milligrams for a given inlet concentration is determined using Eq. (7) [38].

$$q_{total} = \frac{QA}{1000} = \left(\frac{QC_o}{1000}\right) \int_{t=0}^{t=t_{total}} \frac{C_t}{C_o} dt \qquad (7)$$

The total amount of methylene blue pumped into the column m_{total} is calculated using Eq. (8) [40].

$$m_{total} = \frac{C_o Q t_{total}}{1000} \qquad (8)$$

The percentage removal of methylene blue dye is calculated from the ratio of total quantity of methylene blue adsorbed q_{total} to the total amount pumped into the column m_{total} as shown in Eq. (9) [40].

$$\% \, Removal = \left(\frac{q_{total}}{m_{total}}\right) \times 100 \qquad (9)$$

2.4.2. Dynamic modelling of packed-bed column breakthrough

Kinetic modelling is required to predict the dynamic behaviour of the column. Thomas model, Yoon-Nelson model, Bed Depth Service Time (BDST) and Clark model are four commonly used models to analyse the column performance under various process conditions. These models are used to determine breakthrough performance and to calculate the column kinetic parameters as well as the adsorption capacity of the fixed bed column.

2.4.2.1. Thomas model

Thomas model is simple and widely used by several investigators. The Thomas model was derived based on the equation for conservation of mass in a flow system. Further, it assumes the rate driving force in adsorption follows the second-order reversible kinetics and the adsorption equilibrium follows the Langmuir isotherm with no axial dispersion [42,43]. In addition, it also assumes that the constant separation factor is valid for both favourable or non-favourable isotherm [38]. However, it is only applicable when the external and internal diffusion resistances are extremely small in the adsorption process [43,44]. The adsorption rate constant in a continuous column adsorption process and the maximum solid solute concentration on the sorbent was developed based on the expression of Thomas Model as shown in Eq. (10) [45]. The linearized form of the model is expressed in Eq. (11).

$$\frac{C}{C_o} = \frac{1}{1 + \exp\left[K_T\left(\frac{q_o m - C_o V}{Q}\right)\right]} \qquad (10)$$

where K_T = Thomas rate constant (mL/mg min), q_o = Equilibrium adsorbate uptake (mg/g), m = Amount of adsorbent in column (g), C_o = Inlet methylene blue concentration (mg/L), C = Effluent methylene blue concentration (mg/L), V = Effluent Volume (mL) and Q = Flow rate (ml/min)

$$\ln\left(\frac{C_o}{C} - 1\right) = \left(\frac{K_T q_o m}{Q}\right) - \left(\frac{K_T C_o V}{Q}\right) \qquad (11)$$

The values for kinetic coefficient K_T and the adsorption capacity q_o is determined based on a linear plot of $\ln\left(\frac{C_o}{C} - 1\right)$ against t at a given flow rate.

2.4.2.2. Yoon-Nelson model

The Yoon and Nelson model does not require any detailed data on the characteristics of adsorbate, the physical properties of the adsorbent and the type of adsorbent used, therefore it is less complicated compared to the other models [46]. The Yoon and Nelson model assumes that the rate of decrease in the probability of adsorption for each adsorbate molecule is proportional to the probability of adsorbate adsorption and the probability of adsorbate breakthrough on the adsorbent. The experimental data is modelled using the Yoon and Nelson equation for a single

component as shown in Eq. (12) [46]. The linearized form of the model is expressed in Eq. (13).

$$\frac{C}{C_o} = \frac{1}{1+\exp\left[K_{YN}\left(\tau - t\right)\right]} \tag{12}$$

where K_{YN} = Yoon and Nelson rate constant (min^{-1}), C_o = inlet methylene blue concentration (mg/L), C = effluent methylene blue concentration (mg/L), t = breakthrough time (min) and τ = time required for 50% adsorbate breakthrough (min)

$$\ln\left(\frac{C}{C_o - C}\right) = K_{YN}t - K_{YN}\tau \tag{13}$$

The values for K_{YN} and $K_{YN}\tau$ is obtained respectively from the slope and intercept in a $\ln\left(\dfrac{C}{C_o - C}\right)$ vs. t linear plot.

2.4.2.3. BDST model

The BDST model is widely used in comparing the adsorption capacity in adsorption columns under different experimental conditions [41]. BDST model gives the efficiency of the column under constant operating conditions for achieving a desired breakthrough level [47]. It models a linear relationship between the column bed depth and the service time in terms of process concentration and adsorption parameters. Service time is the time required for an adsorbent to adsorb a specific amount of adsorbate from a solution before regeneration is needed [38]. The BDST model physically measures the capacity of the bed at different breakthrough values. BDST model provides useful modelling equations for the changes of system parameters [48]. The experimental data is modelled by BDST based on the Bohart and Adams equation shown in Eq. (14) [47].

$$t = \left(\frac{N_o H_T}{C_o u}\right) - \left(\frac{1}{K_o C_o}\right)\ln\left(\frac{C_o}{C_t} - 1\right) \tag{14}$$

where C_o = inlet solute concentration (mg/L), C_t = effluent concentration of solute in the liquid phase (mg/L), u = influent linear velocity (cm/min), N_o = adsorption capacity (mg/L), K_o = rate constant (L/mg min), t = time (min) and H_T = bed height of column (cm). The value of N_o and K_o is determined respectively from the slope and intercept in a t against bed height H_T plot. The BDST model can be further simplified into Eq. (15).

$$t = az - b \tag{15}$$

where $a = \left(\dfrac{N_o}{C_o u}\right)$ = Slope and $b = \left(\dfrac{1}{K_o C_o}\right)\ln\left(\dfrac{C_o}{C_t} - 1\right)$ = Intercept.

2.4.2.4. Clark model

Clark model was developed by Clark in 1987 [49]. This model is based on the use of a mass-transfer concept in combination with the Freundlich isotherm. Clark model

assumes that the shape of the mass transfer zone is constant and all the adsorbates are removed at the end of the column [50]. Clark model is expressed as per Eq. (16):

$$\left(\frac{C_o}{C_t}\right)^{n-1} - 1 = A\,e^{-rt} \tag{16}$$

where C_0 is the initial MB dye concentration (mg/L), C_t is the MB concentration at time 't', n is the Freundlich constant parameter, A and r (min^{-1}) are Clark constants. The linearized form of Eq. (16) can be expressed as shown below:

$$n\left[\left(\frac{C_0}{C_t}\right)^{n-1} - 1\right] = -rt + \ln A \tag{17}$$

The kinetic model parameters are obtained from the plot of $\ln\left[\left(\dfrac{C_0}{C_t}\right)^{n-1} - 1\right]$ vs. t.

3. Results and discussion

3.1. Characterization of adsorbent

3.1.1. FTIR analysis of mixed packed bed materials

The FT-IR spectrum of pine cone-kaolin mixture before and after MB dye adsorption are shown in Figs. 4 and 5 respectively.

The obtained FTIR results shown in Fig. 4 for pine cone and kaolin mixture before adsorption shows the various functional groups that are responsible for the binding of MB cationic dye to the packed bed adsorbent mixture. The peaks at 3688.5 cm^{-1} and 3619.7 cm^{-1} represent strong O–H stretching free vibrations while the spectra bands observed at 3353.6 cm^{-1} and 2926.2 cm^{-1} are due to O–H stretching Hydrogen-bonded vibrations. The peak at 1610.5 cm^{-1} indicates medium N–H bend with amides while the peak at 1510.4 cm^{-1} represents bending of N–H with amines. Peak at 1446.3 cm^{-1} represents medium C–C=C asymmetric stretch vibrations with aromatic rings. The peaks at 1262.4 cm^{-1}, 1114.2 cm^{-1}, 1028.0 cm^{-1}, 1006.1 cm^{-1} correspond to C–O stretching vibrations to alcohol, esters and ethers. Strong
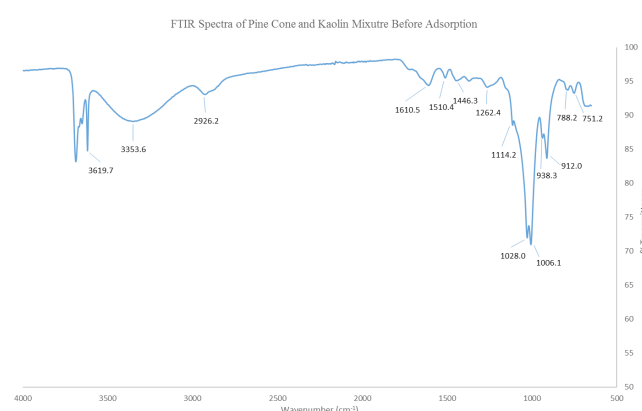
Fig. 4. FTIR Spectra of pine cone and kaolin mixture before adsorption.
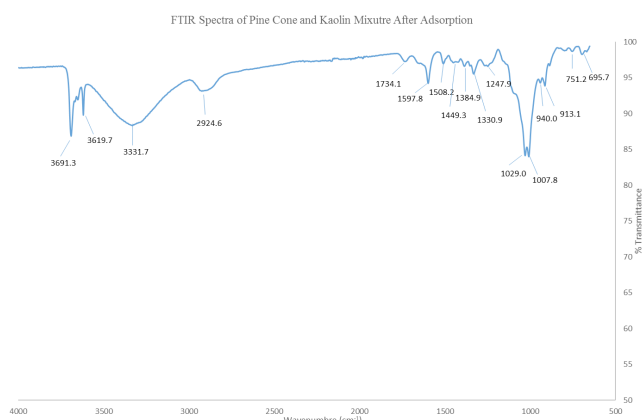
Fig. 5. FTIR spectra of pine cone and kaolin mixture after adsorption.

alkene =C–H bends are assigned to range of 665 cm^{-1} to 990 cm^{-1} at peaks 938.3 cm^{-1}, 912 cm^{-1}, 788.2 cm^{-1} and 751.2 cm^{-1}.

Whereas FTIR results obtained for pine cone and kaolin mixture after adsorption shown in Fig. 5. It was found from Fig. 5 that the various functional groups present in the adsorbent after binding with MB dye molecules. Strong O–H stretching bonds are observed at peaks 3691.3 cm^{-1} and 3619.7 cm^{-1}. Peaks at 3331.7 cm^{-1} and 2924.6 cm^{-1} indicate O–H stretching Hydrogen-bonded vibrations. The peak at 1734.1 is due to strong C=O stretching vibrations while the peaks at 1597.8 cm^{-1} and 1580.2 cm^{-1} represents bending of N–H with amines. Peak at 1446.3 cm^{-1} represents medium C–C=C asymmetric stretch vibrations with aromatic rings. Two strong stretching N–O bands are observed at peaks 1384.9 cm^{-1} and 1330.9 cm^{-1}. The peaks at 1247.9 cm^{-1}, 1029.0cm^{-1} and 1007.8 cm^{-1} correspond to C–O stretching vibrations to alcohol, esters and ethers. Strong alkene =C–H bends are assigned to range of 665 cm^{-1} to 990 cm^{-1} at peaks 940.0 cm^{-1}, 913.1 cm^{-1}, 751.2 cm^{-1} and 695.7 cm^{-1}. The main difference between the FTIR results for adsorbent mixture before and after adsorption is the percentage of transmittance. For example, the peak at 1028 cm^{-1} has increased from 71.95% to 84.15% after adsorption. This indicates that the sample has now adsorbed less radiation from FTIR compared to before. In addition, the appearance of peak 1734.1 cm^{-1} is observed after adsorption, indicating strong C=O stretching vibrations.

3.1.2. Particle sizing and surface area of Pine cone and Kaolin

The surface area of an adsorbent is important because it provides contact area for the binding of adsorbates. It is desirable for an adsorbent to have large surface area because it will lead to a larger area exposed for the binding of adsorbates, and consequently lead to higher adsorption performances [51]. In order to have a large surface area, the particle sizes must be small. Fig. 6 shows the particle size distribution of pine cone and it was found that most of the particles are within the range of 80–100 µm. From Malvern particle sizer, the specific surface area for pine biomass and kaolin were calculated as 0.15 m^2/g and 1.77 m^2/g respectively. The surface weighted mean sizes of pine cone
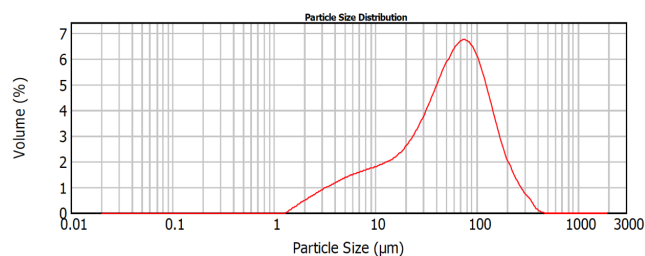
Fig. 6. Particle size distribution of pine cone.

Table 1
Batch adsorption results for different adsorbent mixture proportions

Adsorbent mixture	Amount of dye adsorbed q_t (mg/g)	Dye removal%
4 kaolin : 0 pine cone	9.70	19.40
3 kaolin : 1 pine cone	16.35	32.69
2 kaolin : 2 pine cone	25.07	50.14
1 kaolin : 3 pine cone	33.00	66.00
0 kaolin : 4 pine cone	31.79	63.57

and kaolin particles was found to be 19.65 µm and 3.51 µm respectively.

3.2. Determination of optimum mixing ratio of mixed packed bed adsorbents by MB batch adsorption studies

Batch MB dye adsorption experiments were carried out at different adsorbents mixing ratio as presented in Table 1. Also, from Table 1 it is observed that pine cone biomass has higher MB dye removal capacity compared to pure kaolin with the maximum adsorption capacity of 31.79 mg/g and 9.7 mg/g respectively. Similar trend was observed in the removal of MB dye by previous researchers where pine biomass had q_m of 109.9 mg/g [52] while kaolin had q_m of 75.8 mg/g [53]. It was observed that the adsorbent mixture weight ratio of 3 pine cones: 1 kaolin gives highest amount of MB dye adsorbed qt of 33.0 mg/g and percentage dye removal of 66.0% as shown in Table 1. However, increasing the weight ratio of kaolin from 25% to 75% decreases the adsorption capacity, q_t from 33.0 mg/g to 16.35 mg/g. Pine cone biomass has higher adsorption capacity due to its structural properties [54] while kaolin clay has high cations exchange capacity, chemical and mechanical stability and layered structure [55]. Pine cone biomass contains organic compounds (lignin, cellulose and hemicellulose) with polyphenolic groups that might be strong binding sites for MB adsorption [52], whereas adsorption of MB on clay minerals kaolin is mainly dominated by ion-exchange process i.e. it is highly dependent on solution pH. Therefore in mild acidic solution uptake of MB by kaolin will be less compared to biomass. Moreover, the use of pine cone biomass is feasible because of its abundance in nature, making it relatively cheaper compared to commercially bought kaolin and most importantly sustainable utilization of agricultural solid waste Therefore, the optimum adsorbent weight ratio of 1 kaolin and 3 pine cone

Table 2
Breakthrough curve parameters for the adsorption of MB at different bed heights

h (cm)	t_b (min)	t_{total} (min)	V_{eff} (mL)	q_{total} (mg)	m_{total} (mg)	% Removal	MTZ or H_{UNB} (cm)	H_B (cm)
3	59	112	1678.08	102.19	167.81	60.9	1.42	1.58
5	78	130	1954.92	134.51	195.49	68.8	2.01	2.99
7	98	148	2223.65	153.64	222.36	69.4	2.36	4.64

biomass was chosen in this column study. All experimental measurements are within 10 % accuracy.

3.3. Packed bed column performance at various operating conditions

3.3.1. Effect of mixed adsorbent bed height on BTC

The adsorbent packed bed height has a strong influence on the steepness of the BTC as the column adsorption performance is dependent on the amount of packed adsorbent in the column. To study the effect of bed height on the adsorption of MB, the mixed adsorbent bed height was varied at 3, 5 and 7 cm while the initial MB concentration and flow rate were kept constant. The obtained breakthrough curves for the different bed height are shown in Fig. 7. The breakthrough curve parameters were calculated and then tabulated in Table 2.

It was found from Fig. 7 and Table 2 that the breakthrough time (t_b) increased with an increase in bed height and it was varied from 59 min to 98 min when bed height was increased from 3 to 7 cm. It was also found from Table 2 that the adsorption capacity of mixed bed column was increased from 102.19 to 153.64 mg with the increase of bed height and therefore percentage dye removal was also increased. This is because, as the bed height increases, MB had more contact time with the adsorbent bed, which resulted in a higher removal efficiency of MB molecules in the column. The steepness of the breakthrough curve decreased with increasing bed height due to a higher mass transferring zone [56]. In addition, smaller bed height led to less adsorption site for the binding for MB molecules [57]. It was found that axial dispersion mechanism predominates in the mass transfer for smaller bed heights hence reduced the diffusion of molecules, leading to less time for MB to fully diffuse into the whole adsorbent mass [58]. Higher bed adsorption capacity and better the intra-particulate phenomena is observed at larger bed height.

The results also shows that the breakthrough time increased with increasing bed height. The percentage of MB removal has been increased from 60.9% to 69.4% with the increase of bed height from 3 cm to 5 cm respectively. Higher break through time enables more intra-particle diffusion phenomena, leading to a higher adsorption capacity of the column [47], which is further supported by increase of total quantity of MB adsorbed from 102.19 mg to 153.64 mg which is shown in Table 2. In addition, the length of used bed, H_B, has also increased from 1.58 cm to 4.64 cm, showing higher adsorption capacity of the column. Lastly, larger volume of effluent is treated at higher bed height, which is favourable for industrial scale column adsorption operation. To get the
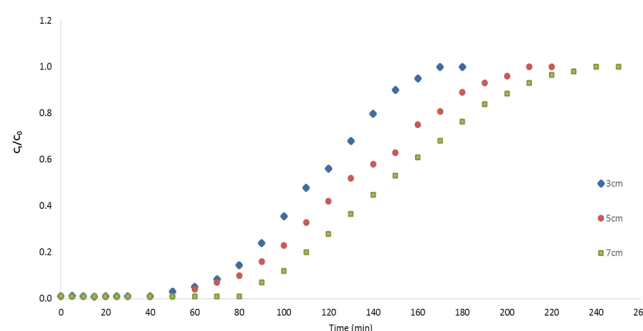
Fig. 7. Breakthrough curves (BTC) for MB adsorption onto pine cone and kaolin mixture for different bed heights (MB flow rate = 15 mL/min, MB dye concentration = 100 ppm and temperature 25±1°C).
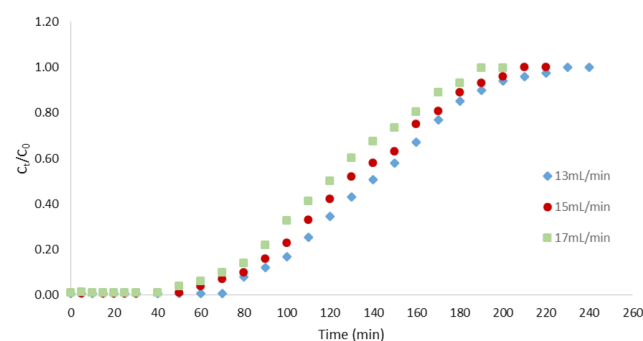
Fig. 8. Breakthrough curves for MB adsorption onto pine cone and kaolin mixture for different flow rates (MB dye concentration = 100 ppm, bed height = 5 cm and temperature 25±1°C).

better performance of mixed packed bed column, higher removal percentage of MB dye and handling of higher volumes of discharge liquid effluents, the height of bed depth should be increased. Similar results were also reported from studies conducted by other researchers [8,38,56,59,60].

3.3.2. Effect of inlet flow rate on BTC

At industrial scaled operations, flow rate is a crucial parameter in assessing the efficiency of adsorbents in a continuous adsorption process. Fig. 8 shows the effect of different flow rates on the breakthrough curves of MB adsorption onto pine cone biomass and kaolin mixture under a packed bed height of 5 cm and an initial MB concentration of 100 ppm. At higher flow rates, the volume of MB sent to the

column was larger, causing more MB molecules to come in contact with the adsorbent bed and leading to a shorter breakthrough time [57]. It is also due to increase of turbulence at higher flow rate decreases the external bulk phase mass transfer resistance to the surface of solid adsorbent and hence the rate of movement of bulk phase MB dye molecules to the surface will be high. This leads to quick saturation and earlier breakthrough time at higher flow rate. Further, the initial phase of adsorption process is fast for all three flow rates, indicating the availability of adsorption sites for the binding of dye molecules around or inside the adsorbent materials. The breakthrough curve is shown to be steeper with increasing flow rate because of the shorter contact time of MB molecules with the mixed-adsorbent bed, which resulted in lower effective adsorption capacity. Thus, higher adsorption was observed at lower flow rates, which resulted in longer breakthrough and exhaustion time.

The breakthrough curve parameters were calculated and then tabulated in Table 3. The results shows that the breakthrough time decreased from 88 min to 59 min for flow rates from 13 mL/min to 17 mL/min. Aside from that, the amount of MB adsorbed decreased with increasing flow rate. This is due to insufficient contact time with the adsorbent bed for intra-particle diffusion, causing MB molecules to leave the adsorption column before achieving equilibrium at higher flow rate [40]. The insufficient residence time of MB molecules in the column has led to an increase in the length of unused bed or mass transferring zone. The length of unused bed has increased from 1.83 cm to 2.55 cm for increasing flow rate. This is further supported by the reduction in the percentage of MB removal from 72.8% to 66.3%. However, the volume of effluent has increased from 1805.20 mL to 2044.37 mL with increasing flow rate of 13 mL/min to 17 mL/min, leading to more MB molecules coming in contact with the adsorbent bed and leading to a faster breakthrough time. These results are agreeable with many earlier reported results [8,38,56,57,59,60]. This results indicated that the lower flow rate is suitable for better performance of packed bed adsorption column but with undesirable overall long processing time for large volume of dye bearing wastewater effluents.

3.3.3. Effect of initial MB dye concentration on BTC

Fig. 9 shows the effect of different initial MB concentration on the breakthrough curves (BTC)of MB adsorption onto mixed adsorbents under a packed bed height of 5 cm and a constant flow rate of 15 mL/min. The breakthrough curves are shown to be slower with lower initial MB concentration due to lower dye removal efficiencies, larger mass transferring zone and film controlled process. The breakthrough curves become

steeper with increasing initial MB concentration, indicating that the change of concentration affects the breakthrough and exhaustion time. It is obvious that the difference in MB concentration between the surface of the adsorbent and the solution is the driving force for adsorption. The amount of MB molecules passing through the column increases at higher initial MB concentration under a fixed time interval, leading to more adsorption sites being occupied and a rise in adsorption capacity [40]. Thus, the lower influent MB concentration resulted in a slower transport due to a smaller concentration gradient leading to smaller reduced mass transfer and diffusion coefficient [48]. However, lower initial MB concentration showed a longer breakthrough time indicating that higher volume of solution could be treated [60].

The breakthrough curve parameters were calculated and tabulated in Table 4. The results show that the breakthrough time decreased from 108 to 59 min with increasing MB concentration of 50 ppm to 150 ppm, whereas the exhaustion time decreased from 163 to 103 min. The MB removal efficiency has increased from 59.4% to 74.0% due to the higher driving force at higher MB concentration [39]. However, the total volume effluent is shown to be higher at lower initial MB concentration, with a total of 2446.61 mL at 50 ppm indicating that more solution could potentially be treated. At higher initial MB concentration, the breakthrough curves are shown to be steeper, illustrating a smaller mass transferring zone and intra-particle diffusion controlled process. This is further supported by the increase in length of used bed (H_B) at higher initial MB concentration. Therefore, it is proven that the diffusion process is dependent on concentration. The column study for 50 ppm initial MB concentration has a percentage removal of 59.4%, which is lower compared to the previous batch study for the same initial dye concentration with 66% of MB removal as shown in Table 1. This could be due to insufficient con-
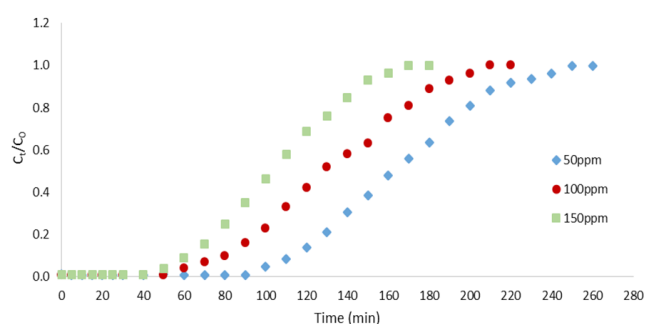
Fig. 9. Breakthrough curves for MB adsorption onto pine cone and kaolin mixture for different initial MB concentrations(flow rate = 15mL/min, bed height = 5 cm and temperature 25±1°C).

Table 3
Breakthrough curve parameters for the adsorption of MB under different flow rates

Q (mL/min)	t_b (min)	t_{total} (min)	V_{eff} (mL)	q_{total} (mg)	m_{total} (mg)	% MB removal	MTZ or H_{UNB} (cm)	H_B (cm)
13	88	139	1805.20	131.48	180.52	72.8	1.83	3.17
15	78	130	1954.92	134.51	195.49	68.8	2.01	2.99
17	59	120	2044.37	135.56	204.44	66.3	2.55	2.45

Table 4
Breakthrough curve parameters for the adsorption of MB under different initial MB concentrations

C_0 (mg/L)	t_b (min)	t_{total} (min)	V_{eff} (mL)	q_{total} (mg)	m_{total} (mg)	% MB Removal	MTZ or H_{UNB} (cm)	H_B (cm)
50	108	163	2446.61	72.67	122.33	59.4	1.69	3.31
100	78	130	1954.92	134.51	195.49	68.8	2.01	2.99
150	59	103	1551.80	172.23	232.77	74.0	2.16	2.84

tact time between the adsorbent bed and the MB adsorbate. Similar trends were also obtained for the removal of phenol using palm shells [57], the adsorption of MB onto rice husk [48], oil palm shells [60], phoenix tree leaf powder [56], eucalyptus bark [8] and pine cone [38]. It can be concluded from this study that higher MB concentration is favourable for better performance of packed bed adsorption column.

3.4. Dynamic modelling of pine cone-kaolin packed bed column

3.4.1. Application of Thomas model

The column experimental data from breakthrough curve were fitted against the Thomas model to calculate its maximum solid-phase MB concentration (q_o) and the Thomas kinetic rate constant (K_{th}) The model parameters and linear correlation coefficient (R^2) were determined using the linear regression analysis based on Eq. (10). The predicted linear plots of $\ln[(C_o - C_t) - 1]$ against time (t) under different bed heights (3, 5 and 7 cm), MB flow rates (13, 15 and 17 mL/min) and initial MB concentrations (50, 100 and 150 ppm) according to the Thomas model are shown in Fig. 10a, b and c respectively. The values of K_{th} and q_o are determined based on the slope and intercept of the plots respectively.

The calculated model parameters and correlation coefficients are tabulated in Table 5. Higher linear regression coefficient (R^2) value indicates the applicability of Thomas model (Table 5) and adsorption follows Langmuir isotherm model which indicates the formation of monolayer on adsorbent surface. It was found from Table 5 that with the increasing bed heights from 3 cm to 7 cm, the K_{th} values decreased from 0.562 mL/min·mg to 0.425 mL/min·mg and the q_o values increased from 20.19 mg/g to 35.96 mg/g. This is due to the wider spread of MB dye adsorbed onto the adsorbent bed, ensuring that most MB will diffuse into the adsorbent bed before leaving the column. Under varying flow rate from 13 mL/min to 17 mL/min, the value of K_{th} is shown to increase from 0.425 mL/min·mg to 0.430 mL/min·mg while the maximum solid-phase concentration decreased from 26.50 mg/g to 22.98 mg/g due to the higher amount of MB dyes being pumped through the same amount of adsorbent bed at higher flow rate. The increase in K_{th} values at higher flow rates are due to the faster mass transfer [61]. Faster mass transfer might be due to the macro pores of the adsorbent [62]. Besides that, higher flow rate has led to a lower adsorption capacity due to the insufficient residence time of the MB molecules in the column and diffusion into the pores of the adsorbent. Thus, the MB molecules left the column before achieving equilibrium [63]. At higher initial MB concentration, the K_{th} values are shown to be decreasing while q_o values are increasing. This is because, the MB concentration gradient between the sur-
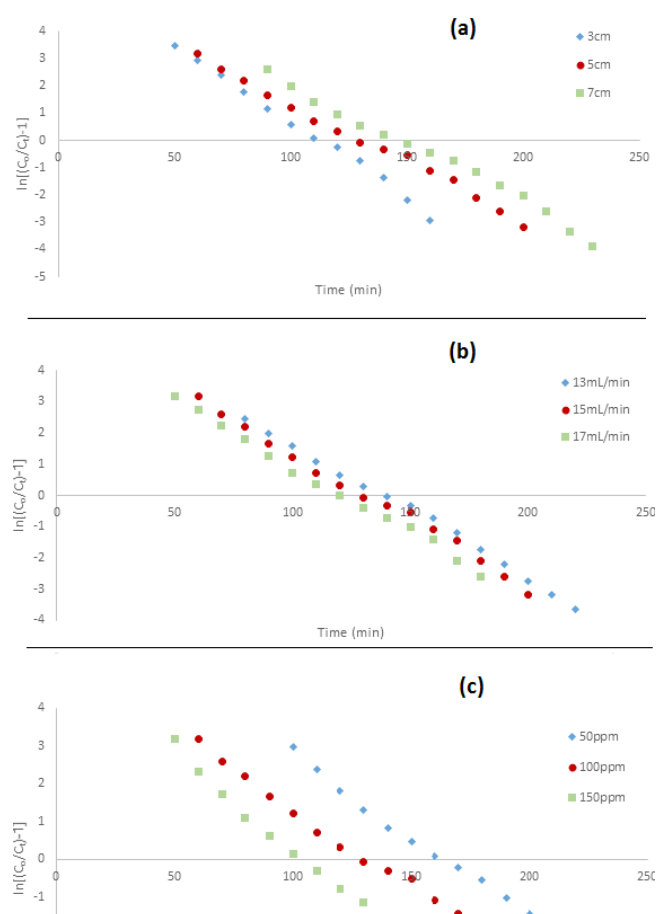
Fig. 10. Thomas kinetic plot for adsorption of MB onto pine cone and kaolin mixture: (a) effect of bed height (flowrate = 15 mL/min, inlet MB concentration = 100 ppm and temperature 25±1°), (b) effect of flow rate (bed height = 5 cm, inlet MB concentration = 100 ppm and temperature 25±1°), (c) effect of initial MB concentration (flow rate = 15 mL/min, bed height = 5 cm and temperature 25±1°).

face of the adsorbent and the solution is the driving force for adsorption [39]. The external and internal diffusion will not be the limiting step because the experimental data fitted well with the Thomas model [41]. Hence, the column performance was found better at higher MB initial concentration due to the higher adsorption driving force. In short, higher adsorbent bed height, lower MB solution flow rate and higher MB initial concentration would lead to better performance of pine cone-kaolin mixed packed bed column in the removal of methylene blue (MB) dye. Similar results for different systems were also obtained [40,57,64,65].

Table 5
Kinetic parameters of Thomas model under various experimental conditions

	Bed height (cm)			Flow rate (mL/min)			Initial MB concentration (mg/L)		
Thomas model	3	5	7	13	15	17	50	100	150
K_{Th} (mL/min·mg)	0.562	0.427	0.425	0.425	0.427	0.428	0.848	0.427	0.360
q_o (mg/g)	20.19	25.12	35.96	26.50	25.12	22.98	15.77	25.12	29.97
R^2	0.995	0.994	0.990	0.996	0.994	0.995	0.996	0.994	0.992

3.6.2. Application of Yoon-Nelson model

The experimental data were also fitted against a simple theoretical model developed by Yoon-Nelson in studying the breakthrough behaviour of MB dye onto mixture of pine cone biomass and kaolin. The parameters for Yoon-Nelson constant (K_{YN}) and τ (the time required for 50% sorbate breakthrough) were determined from linear regression with a linear plot $\ln[C_t / (C_o - C_t)]$ of against time under various experimental conditions (different adsorbent bed heights, different MB flow rates and different initial MB concentrations) according to Eq. (13). The values of K_{YN} and τ are calculated based on the slop and intercept of the straight line plots shown in Fig. 11a, b and c respectively. The calculated model fitted kinetic parameters for Yoon-Nelson model are presented in Table 6. With increasing bed height, the 50% breakthrough time τ is shown to be increased and the K_{YN} values decreased. The Yoon-Nelson constant K_{YN} was found to increase while the 50% breakthrough time decreased at higher initial MB concentration and flow rate. K_{YN} value increased from 0.0426 min⁻¹ to 0.0540 min⁻¹ while τ decreased from 163.9 min to 104 min at MB concentration of 50 ppm to 150 ppm. Infact increase in MB concentration causes adsorbate molecules to compete for available adsorption sites, leading to an increase in uptake rate [56,66]. The obtained high value of linear regression coefficients (R^2) indicates the applicability of this model. In addition, the time required for 50% adsorbate breakthroughs τ from Yoon-Nelson model were agreeable with the obtained experimental data. Similar trends of results were also reported by other researchers [40,41,61,67].

3.6.3. Application of BDST model

BDST model was also applied to the column data obtained from MB adsorption by pine cone biomass and kaolin mixture under different bed heights to determine its adsorption capacity and kinetic constant. A linear plot of total column service time against the bed height according to the BDST model is shown in Fig. 12. Column service time, also known as the exhaustion time is the time taken for all the active binding site of an adsorbent to become fully occupied by adsorbate molecules until regeneration is required.

Thus, the exhaustion times for of the column adsorption at bed heights 3, 5 and 7 cm, at a constant flow rate of 15 mL/min and 100 ppm initial MB concentration were recorded. Based on Fig. 12, it can be seen that the experimental data fitted well with BDST model, having a high correlation coefficient R^2 of 0.993. The model parameters of N_o and K_o are listed in Table 7 which are calculated based on the slope and the intercept of the plot respectively. N_o is cal-
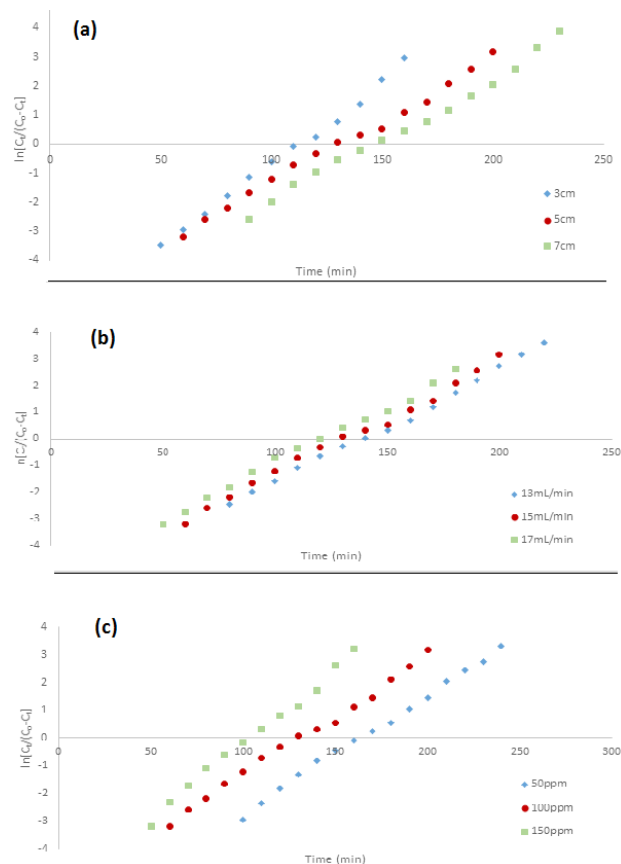
Fig. 11. Yoon-Nelson kinetic plot for adsorption of MB onto pine cone and kaolin mixture (a)effect of bed height (flow rate = 15 mL/min, inlet MB concentration = 100 ppm and temperature 25±1°), (b) effect of flow rate (bed height = 5 cm, inlet MB concentration = 100 ppm and temperature 25±1°), (c) effect of initial MB concentration (flow rate = 15 mL/min, bed height = 5 cm and temperature 25±1°).

culated by assuming constant initial MB concentration (C_o) and linear velocity (v) of MB flowing through the column due to the uniform column diameter and constant MB volumetric flow rate. The calculated model rate constant (K_o) represents the rate of solute transfer from the fluid to the solid phase [68]. The values for N_o and K_o are 5347.61 mg/L and 0.505 L/mg·min respectively. The breakthrough time is found to be dependent on the K_o value. In general, a short adsorbent bed is sufficient enough to prolong breakthrough at large K_o value, whereas small K_o value will require longer adsorbent bed to avoid breakthrough [68]. The BDST model can be used to predict slope for any unknown flow rate with

Table 6
Kinetic parameters of Yoon-Nelson model under various experimental conditions

	Bed height (cm)			Flow rate (mL/min)			Initial MB concentration (mg/L)		
Yoon- Nelson model	3	5	7	13	15	17	50	100	150
$K_{YN} \times 10^2$ (min^{-1})	5.64	4.27	4.25	4.25	4.27	4.30	4.26	4.27	5.40
τ (min)	112.1	130.7	147.0	138.0	130.7	121.4	163.9	130.7	104.0
$\tau_{50\%,exp}$ (min)	102.9	117.9	136.0	127.4	117.9	108.6	149.7	117.9	93.2
R^2	0.995	0.994	0.990	0.996	0.994	0.995	0.996	0.994	0.992
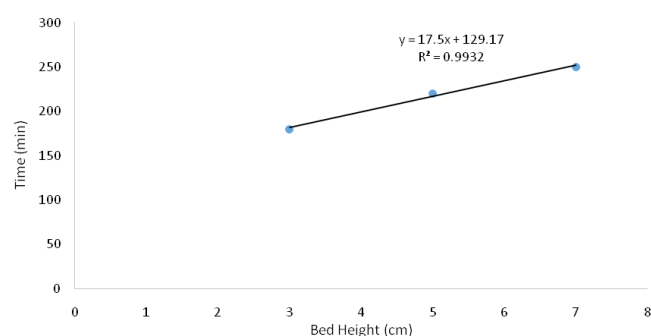
Fig. 12. Bed depth service time (BDST) kinetic plot for adsorption of MB onto pine cone and kaolin mixture at different bed heights (flow rate = 15 mL/min, inlet MB concentration = 100 ppm and temperature 25±1°).

a known slope at a given flow rate. Therefore, it is useful in scaling up the process for other flow rates and concentrations without the need of further experimental runs [48].

3.6.4. Application of Clark model

The column experimental data from breakthrough curve were fitted against the Clark model where the figures are not presented here. Clark model uses Freundlich constant to simulate the modelling of the breakthrough curves in fixed bed adsorption. However, Freundlich constant, '*n*' was determined from our earlier MB batch isotherm experiments on pine cone and kaolin adsorbents and it was found to be above unity which indicates favourable adsorption for both the systems [52,53]. Therefore the value of '*n*' was taken as 1.5 in Clark model parameters calculation. The experimental data from breakthrough curve (BTC) were applied to Eq. (17) and the values of *A* and *r* (min^{-1}) in the Clark model were determined as shown in Table 8. It was found that *r* (min^{-1}) was decreasing from 0.036 to 0.029 with the increases of bed height from 3 to 7 cm and increasing from 0.026 to 0.039 with the increases of initial MB dye concentration from 50 to 150 mg/L. However, the *r* (min^{-1}) was constant (0.031) across various MB dye flow rates. The constant A was shown to increase from 19.61 to 24.94 with the increases of bed height and decrease in the increases of flow rate and initial dye concentration. Furthermore, the linear regression coefficient (R^2) were found to be above 0.91 under various operation parameters which indicates the applicability of Clark model as shown in Table 8.

3.6.5. Summary of calculated kinetic parameters for Thomas, Yoon-Nelson, BDST and Clark models

Table 7
BDST-model parameters for adsorption of MB onto mixture of pine cone biomass and kaolin clay

Adsorbent	N_o (mg/L)	K_o (L/mg·min)	R^2
3 pine cone: 1 kaolin mixture	5347.61	0.505	0.993

4. Conclusion

In conclusion, this study confirmed the suitability of pine cone biomass and kaolin clay mixture as alternative adsorbents for the continuous adsorption of MB dye from aqueous solution in a packed bed column. The use of two low cost adsorbents in a continuous adsorption column operation gives the process more commercially viable option. The optimum adsorbents mixing ratio was determined by batch adsorption method. Therefore, all column adsorption experiments were conducted with the obtained optimum mixed adsorbents packed bed materials. The BTCs for MB removal were analysed under varying bed height, flow rate and initial MB concentration. The adsorbent bed height, the feed flow rate and the initial MB dye concentration have shown strong influence on the adsorption of MB in a continuous operation. Column performances were enhanced at higher bed height, higher initial Mb dye concentration and at lower inlet flow rate. Based on the column results obtained, it shows that higher adsorbent bed height led to a higher MB adsorption and a longer breakthrough time. This is because of higher adsorbent bed height enables more intra-particle diffusion phenomena, leading to a higher adsorption capacity of the column. Whereas, higher flow rates led to a lower MB adsorption and faster breakthrough time. This is due to the insufficient contact time of the MB molecules with the adsorbent bed for intra-particle diffusion, causing MB molecules to leave the adsorption column before achieving equilibrium. The removal of MB increased with increasing initial MB concentration. The highest MB removal was obtained at the highest initial MB concentration due to the high adsorption driving force. It is found that higher initial methylene blue concentration with lower flow rate and higher bed depth gives better column adsorption performance. This is because at lower flow rate and higher bed depth, the contact time is longer while at higher initial MB concentration, the driving force for adsorption is higher. In general, the interaction between MB molecules and the adsorbent mixture is the main influence for the adsorption performance in the column. The experimental data were then fitted against Thomas, Yoon-Nelson, BDST and Clark models to anal-

Table 8
Clark model parameters for adsorption of MB onto mixture of pine cone biomass and kaolin

	Bed height (cm)			Flow rate (mL/min)			Initial MB concentration (mg/L)		
Clark model	3	5	7	13	15	17	50	100	150
r (min^{-1})	0.036	0.031	0.029	0.031	0.031	0.031	0.026	0.031	0.039
A	19.61	19.81	24.94	24.76	19.81	15.85	24.04	19.81	20.23
R^2	0.945	0.967	0.929	0.948	0.967	0.971	0.913	0.967	0.964

yse the column performance in the removal of methylene blue dye. Results from the Thomas model revealed that the value of maximum solid phase concentration (q_o) increased with increasing bed height and initial MB concentration but decreased with flow rate. The value of Thomas rate constant (K_{Th}) increased with increasing flow rate but decreased as the bed height and initial MB concentration increased. The application of Yoon-Nelson model showed that the time required for 50% adsorbate breakthrough (τ) were compatible with the experimental data ($\tau_{50\%,exp}$). Besides that, the value of Yoon-Nelson rate constant decreased as the bed height increased but increased with both increasing flow rate and initial MB concentration. The bed sorption capacity (N_o) was found to be 5347.6 mg/L for the adsorption of MB onto pine cone and kaolin mixture according to the BDST model. The high value of linear regression coefficient (R^2) of Clark model fitting with experimental BTC indicates the applicability of this model. Therefore, all four kinetic models were shown successful in predicting the BTC with high correlation coefficients. It is obvious that the characteristic parameters of these models are different but they predict essentially the same uptake capacity and values for a given experimental data set. However, the unique and prominent characteristic feature of each models such as the adsorption capacity for Thomas model, the time for 50% breakthrough in Yoon-Nelson model and the service time for BDST model enables further comparison. Therefore, the characteristic of each model were calculated based on the model's predicted equations in this present study. This study indicates that the mixture of pine cone biomass and kaolin clay has a strong adsorption capacity and can be recognised as an alternative sustainable solution for dye-bearing wastewater treatment.

References

[1] S.C.R. Santos, R.A.R. Boaventura, Adsorption of cationic and anionic azo dyes on sepiolite clay: Equilibrium and kinetic studies in batch mode, J. Env. Chem. Eng., 4 (2016) 1473–1483.

[2] S. Afroze, T.K. Sen, M. Ang, H. Nishioka, Adsorption of methylene blue dye from aqueous solution by novel biomass Eucalyptus sheathiana bark: equilibrium, kinetics, thermodynamics and mechanism, Desal. Water Treat., 57 (2015) 5858–5878.

[3] S. De Gisi, G. Lofrano, M, Grassi, M. Notarnicola, Characteristics and adsorption capacities of low-cost sorbents for wastewater treatment: A review, Sustain. Mat. Tech., 9 (2016) 10–40.

[4] M.T. Yagub, T.K. Sen, S. Afroze, H.M. Ang, Fixed-bed dynamic column adsorption study of Methylene Blue (MB) onto pine cone, Desal. Water Treat., 55 (2014) 1026–1039.

[5] S. Dawood, T.K. Sen, C. Phan, Adsorption removal of Methylene Blue (MB) dye from aqueous solution by bio-char prepared from Eucalyptus sheathiana bark: kinetic, equilibrium, mechanism, thermodynamic and process design, Desal. Water Treat., 57(59) (2016) 28964–28980.

[6] S. Dawood, T.K. Sen, Review on dye removal from its aqueous solution into alternative cost effective and non-conventional adsorbents, J. Chem. Proc. Eng., 1 (2014) 1–7.

[7] T. Chiong, S.Y. Lau, Z.H. Lek, B.Y. Koh, M.K. Danquah, Enzymatic treatment of methyl orange dye in synthetic wastewater by plant-based peroxidase enzymes, J. Env. Chem. Eng., 4 (2016) 2500–2509.

[8] S. Afroze, T.K. Sen, H.M. Ang, Adsorption performance of continuous fixed bed column for the removal of Methylene Blue (MB) dye using Eucalyptus sheathiana barkbiomass, Springer, (2015) 1–22.

[9] I. Arslan, I.A. Balcioğlu, D.W. Bahnemann, Advanced chemical oxidation of reactive dyes in simulated dyehouse effluents by ferrioxalate-Fenton/UV-A and TiO$_2$/UV-A processes, Dyes Pig., 47 (2000) 207–218.

[10] I. Nilsson, A. Möller, B. Mattiasson, M.S.T Rubindamayugi, U. Welander, Decolorization of synthetic and real textile wastewater by the use of white-rot fungi, Enzy. Micro. Tech., 38 (2006) 94–100.

[11] T. Sauer, G. Cesconeto Neto, H.J. José, R.F.P.M. Moreira, Kinetics of photocatalytic degradation of reactive dyes in a TiO$_2$ slurry reactor, J. Photochem. Photobio. A: Chem., 149 (2002) 147–154.

[12] K.V. Kumar, A. Kumaran, Removal of methylene blue by mango seed kernel powder, Biochem. Eng. J., 27 (2005) 83–93.

[13] X. Quan, D. Luo, J. Wu, R. Li, W. Cheng, S. Ge, Ozonation of acid red 18 wastewater using O$_3$/Ca(OH)$_2$ system in a micro bubble gas-liquid reactor, J. Env. Chem. Eng., 5 (2017) 283–291.

[14] P. Navarro, J.A. Gabaldón, V.M. Gómez-López, Degradation of an azo dye by a fast and innovative pulsed light/H$_2$O$_2$ advanced oxidation process, Dyes Pig., 136 (2017) 887–892.

[15] T. Li, X. Hu, C. Liu, C. Tang, X. Wang, S. Luo, Efficient photocatalytic degradation of organic dyes and reaction mechanism with Ag$_2$CO$_3$/Bi$_2$O$_2$CO$_3$ photocatalyst under visible light irradiation, J. Mole. Cat. A: Chem., 425 (2016) 124–135.

[16] R. Yang, H. Li, M. Huang, H. Yang, A. Li, A review on chitosan-based flocculants and their applications in water treatment, Water Res., 95 (2016) 59–89.

[17] K. Anoop Krishnan, K.G. Sreejalekshmi, V. Vimexen, V.V. Dev, Evaluation of adsorption properties of sulphurised activated carbon for the effective and economically viable removal of Zn(II) from aqueous solutions, Ecotox. Env.Safe., 124 (2016) 418–425.

[18] S. Dawood, T.K. Sen, C. Phan, Synthesis and characterisation of novel-activated carbon from waste biomass pine cone and its application in the removal of congo red dye from aqueous solution by adsorption, Water Air Soil Pollut., 225 (2014) 1–16.

[19] M.K. Uddin, A review on the adsorption of heavy metals by clay minerals, with special focus on the past decade, Chem. Eng. J., 308 (2017) 438–462.

[20] M.T. Yagub, T.K. Sen, S. Afroze, H.M. Ang, Dye and its removal from aqueous solution by adsorption: A review, Adv. Colloid. Interface. Sci., 209 (2014) 172–184.

[21] S. Dawood, T.K. Sen, Removal of anionic dye Congo red from aqueous solution by raw pine and acid-treated pine cone powder as adsorbent: Equilibrium, thermodynamic, kinetics, mechanism and process design, Water Res., 46 (2012) 1933–1946.

[22] V.S. Mane, P.V. Vijay Babu, Kinetic and equilibrium studies on the removal of Congo red from aqueous solution using Eucalyptus wood (Eucalyptus globulus) saw dust, J. Taiwan Instit. Chem. Eng., 44 (2013) 81–88.

[23] S. Afroze, T.K. Sen, M. Ang, H. Nishioka, Adsorption of methylene blue dye from aqueous solution by novel biomass Eucalyptus sheathiana bark: equilibrium, kinetics, thermodynamics and mechanism, Desal. Water Treat., 57 (2016) 5858–5878.

[24] L. Borah, M. Goswami, P. Phukan, Adsorption of methylene blue and eosin yellow using porous carbon prepared from tea waste: Adsorption equilibrium, kinetics and thermodynamics study, J. Env. Chem. Eng., 3 (2015) 1018–1028.

[25] M. Kaur, M. Datta, Adsorption equilibrium and kinetics of toxic dye-Erythrosine B adsorption onto Montmorillonite, Sep. Sci. Tech., 48 (2013) 1370–1381.

[26] D.M. El-Mekkawi, F.A. Ibrahim, M.M. Selim, Removal of methylene blue from water using zeolites prepared from Egyptian kaolins collected from different sources, J. Env. Chem. Eng., 4 (2016) 1417–1422.

[27] K. Rida, S. Bouraoui, S. Hadnine, Adsorption of methylene blue from aqueous solution by kaolin and zeolite, Appl. Clay Sci., 84 (2013) 99–105.

[28] B.K. Nandi, A. Goswami, M.K. Purkait, Adsorption characteristics of brilliant green dye on kaolin, J. Hazard. Mat., 161 (2009) 387–395.

[29] B.K. Nandi, A. Goswami, M.K. Purkait, Removal of cationic dyes from aqueous solutions by kaolin: Kinetic and equilibrium studies, Appl. Clay Sci., 42 (2009) 583–590.

[30] V. Vimonses, S. Lei, B. Jin, C.W.K. Chow, C. Saint, Adsorption of congo red by three Australian kaolins, Appl. Clay Sci., 43 (2009) 465–472.

[31] O. Yavuz, C. Saka, Surface modification with cold plasma application on kaolin and its effects on the adsorption of methylene blue, Appl. Clay Sci., 85 (2013) 96–102.

[32] T.S. Anirudhan, M. Ramachandran, Adsorptive removal of basic dyes from aqueous solutions by surfactant modified bentonite clay (organoclay): Kinetic and competitive adsorption isotherm, Pro. Saf. Env. Protec., 95 (2015) 215–225.

[33] K. Chinoune, K. Bentaleb, Z. Bouberka, A. Nadim, U. Maschke, Adsorption of reactive dyes from aqueous solution by dirty bentonite, Appl. Clay Sci., 123 (2016) 64–75.

[34] K. Li, P. Li, J. Cai, S. Xiao, H. Yangand A. Li, Efficient adsorption of both methyl orange and chromium from their aqueous mixtures using a quaternary ammonium salt modified chitosan magnetic composite adsorbent, Chemosphere,154 (2016) 310–318.

[35] H. Yan, H. Yang, A. Li, R. Cheng, pH-tunable surface charge of chitosan/graphene oxide composite adsorbent for efficient removal of multiple pollutants from water, Chem. Eng. J., 284 (2016) 1397–1405.

[36] R. Zhu, Q. Chen, Q. Zhou, Y. Xi, J. Zhu, H. He, Adsorbents based on montmorillonite for contaminant removal from water: A review, Appl. Clay Sci., 123 (2016) 239–258.

[37] M.T. Yagub, T.K. Sen, H.M. Ang, Removal of organic contaminants by natural pine cone and pine leaves as adsorbent, Proceed. CHEMECA Conf.,Syd.: Eng. Aus., (2011) 11.

[38] M.T. Yagub, T.K. Sen, S. Afroze, H.M. Ang, Fixed-bed dynamic column adsorption study of Methylene Blue (MB) onto pine cone, Desal. Water Treat., 55 (2014) 1026–1039.

[39] M.H. Ehrampoush, G.R. Moussavi, M.T. Ghaneian, S. Rahimi, M. Ahmadian, Removal of Methylene Blue (MB) dye from textile synthetic wastewater using TiO$_2$/UV0C Photocatalytic Process, Aust. J. Basic Appl. Sci., 4 (2010) 4279–4285.

[40] T. Ataei-Germi, A. Nematollahzadeh, Bimodal porous silica microspheres decorated with polydopamine nano-particles for the adsorption of methylene blue in fixed-bed columns, J. Collod. Inter. Sci., 470 (2016) 172–182.

[41] S.S. Baral, N. Das, T.S. Ramulu, S.K. Sahoo, S.N. Das, G.R. Chaudhury, Removal of Cr(VI) by thermally activated weed Salvinia cucullata in a fixed-bed column, J. Hazard. Mater., 161 (2009) 1427–1435.

[42] M. Ghasemi, A.R. Keshtkar, R. Dabbagh, S. Jaber Safdari, Biosorption of uranium(VI) from aqueous solutions by Ca-pretreated Cystoseira indica alga: Breakthrough curves studies and modeling, J. Hazard. Mater., 189 (2011)141–149.

[43] R. Han, D. Ding, Y. Xu, W. Zou, Y. Wang, Y. Li, L. Zou, Use of rice husk for the adsorption of congo red from aqueous solution in column mode, Bio. Tech., 99 (2008) 2938–2946.

[44] Z. Xu, J.G. Cai, B.C. Pan, Mathematically modelling fixed-bed adsorption in aqueous systems, J. Zhejiang Uni. Sci. A (Appl. Physc. & Eng.), 14 (2013) 155–176.

[45] H.C. Thomas, Heterogeneous ion exchange in a flowing system, J. Amer. Chem. Soc., 66 (1944) 1664–1666.

[46] Y.H. Yoon, J.H. Nelson, Application of gas adsorption kinetics I. A theoretical model for respirator cartridge service life, Amer. Indust. Hyg. Assoc. J., 45 (1984) 509–516.

[47] S. Sadaf, H.N. Bhatti, Evaluation of peanut husk as a novel, low cost biosorbent for the removal of Indosol Orange RSN dye from aqueous solutions: batch and fixed bed studies, Clean Tech. Env. Pol., 16 (2014) 527–544.

[48] R. Han, Y. Wang, W. Yu, W. Zou, J. Shi, H. Liu, Biosorption of methylene blue from aqueous solution by rice husk in a fixed-bed column, J. Hazard. Mater., 141 (2007) 713–718.

[49] N.N. Clark, C.M. Atkinson, R.L.C. Flemmer, Turbulent circulation in bubble columns, AIChE J., 33 (1987) 515–518.

[50] P. Dhanasekaran, P.M. Satya Sai, K.I. Gnanasekar, Fixed bed adsorption of fluoride by Artocarpus hirsutus based adsorbent, J. Fluorine Chemist., 195 (2017) 37–46.

[51] S. Kara, C. Aydiner, E. Demirbas, M. Kobya, N. Dizge, Modeling the effects of adsorbent dose and particle size on the adsorption of reactive textile dyes by fly ash, Desalination, 212 (2007) 282–293.

[52] M.T. Yagub, T.K. Sen, M. Ang, Removal of cationic dye methylene blue (MB) from aqueous solution by ground raw and base modified pine cone powder, Env. Earth Sci., 71 (2014) 1507–1519.

[53] S. Dawood, T. Gupta, Sen, T.K., Adsorptive removal of Methylene Blue (MB) dye at Kaolin clay-water interface: kinetics, isotherm modelling and process design, in Clay Minerals: Properties, Occurrence and Uses, Nova, (2017) 209–236.

[54] G. Blázquez, M.A. Martín-Lara, E. Dionisio-Ruiz, G. Tenorio, M. Calero, Copper biosorption by pine cone shell and thermal decomposition study of the exhausted biosorbent, J. Indust. Eng. Chem., 18 (2012) 1741–1750.

[55] F. Aries, T.K. Sen, Removal of zinc metal ion (Zn2þ) from its aqueous solution by kaolin clay mineral: a kinetic and equilibrium study, Colloid. Surf., 348 (2009) 100–108.

[56] R. Han, Y. Wang, X. Zhao, Y. Wang, F. Xie, J. Cheng, M. Tang, Adsorption of methylene blue by phoenix tree leaf powder in a fixed-bed column: experiments and prediction of breakthrough curves, Desalination, 245 (2009) 284–297.

[57] A. Garba, N.S. Nasri, H. Basri, R. Ismail, Z.D. Abdul Majid, U. Hamza, J. Mohammed, Adsorptive removal of phenol from aqueous solution on a modified palm shell-based carbon: fixed-bed adsorption studies, Desal. Water Treat., 57 (2016) 488–499.

[58] V.C. Taty-Costodes, H. Fauduet, C. Porte, Y.S. Ho, Removal of lead (II) ions from synthetic and real effluents using immobilized Pinus sylvestris sawdust: Adsorption on a fixed-bed column, J. Hazard. Mater., 123 (2005) 135–144.

[59] N. Mohammed, N. Grishkewich, H.A. Waeijen, R.M. Berry, K.C. Tam, Continuous flow adsorption of methylene blue by cellulose nanocrystal-alginate hydrogel beads in fixed bed columns, Carbo. Polym., 136 (2016) 1194–1202.

[60] I.A.W. Tan, A.L. Ahmad, B.H. Hameed, Adsorption of basic dye using activated carbon prepared from oil palm shell: batch and fixed bed studies, Desalination, 225 (2008) 13–28.

[61] W. Zhang, L. Dong, H. Yan, H. Li, Z. Jiang, X. Kan, H. Yang, A. Li, R. Cheng, Removal of methylene blue from aqueous solutions by straw based adsorbent in a fixed-bed column, Chem. Eng. J., 173 (2011) 429–436.

[62] M.J. Reber, D. Bruhwiler, Bimodal mesoporous silica with bottleneck pores, Dalton Trans., 44 (2015) 17960–17967.

[63] K.S. Bharathi, S.P.T. Ramesh, Fixed-bed column studies on biosorption of crystal violet from aqueous solution by Citrullus lanatus rind and Cyperus rotundus, Appl. Water Sci., 3 (2013) 673–687.

[64] Z.Z. Chowdhury, S.B. Abd Hamid, S.M. Zain, Evaluating design parameters for breakthrough curve analysis and kinetics of fixed bed columns for Cu(II) cations using lignocellulosic wastes, BioRes., 10 (2015) 732–749.

[65] Z. Chowdhury, S. Zain, A. Rashid, R. Rafique, K. Khalid, Breakthrough curve analysis for column dynamics sorption of Mn (II) ions from wastewater by using Mangostana garcinia peel-based granular-activated carbon, J. Chem., 2013 (2013) 8.

[66] O. Hamdaoui, Dynamic sorption of methylene blue by cedar sawdust and crushed brick in fixed bed columns, J. Hazard. Mater., 138 (2006) 293–303.

[67] R. Sharma, B. Singh, Removal of Ni (II) ions from aqueous solutions using modified rice straw in a fixed bed column, Bioresource Tech., 146 (2013) 519–524.

[68] S.H. Hasan, D. Ranjan, M. Talat, Agro-industrial waste 'wheat bran' for the biosorptive remediation of selenium through continuous up-flow fixed-bed column, J. Hazard. Mater., 181 (2010) 1134–1142.